Coupling of Sommerfeld waves using odd TM mode of double-dielectric-slab waveguide

Jia-Min Liu · Hua-Wei Liang · Min Zhang · Hong Su

College of Electronic Science and Technology, Shenzhen University, Shenzhen, 518060, China

Shenzhen Key Laboratory of Laser Engineering, Shenzhen University, Shenzhen, 518060, China

Key Laboratory of Advanced Optical Precision Manufacturing Technology of Guangdong Higher Education Institutes, Shenzhen University, Shenzhen, 518060, China

e-mail:hwliang@szu.edu.cn

Abstract: We report the coupling of cylindrical metal wire THz surface plasmon-polaritons using odd TM mode of double-dielectric-slab waveguide. We analyze the mode matching issue. We calculate the coupling efficiency of the double-dielectric-slab waveguide to copper wire of 1 mm diameter with respect to waveguide structure, beam structure and the THz frequency, theoretically. It is concluded that at 4.2 THz the highest coupling efficiency achieved to be is 43.5%. We further show the coupling experimental system.

Keywords Surface plasmon · Infrared, far · Waveguides · Waveguides, planar

1. Introduction

Terahertz (THz) wave which is locating between the infrared and microwave bands in the electromagnetic spectrum is one of the hot research topics. In recent years, THz technology has shown potential applications in many fields such as sensing, imaging, and spectroscopy. However, THz wave cannot transmit in the free space effectively, so that the waveguide for THz wave is very important. In 2004, Wang and Mittleman [1] reported that a simple metal wire can effectively guide THz wave as surface plasmon-polaritons (SPPs). Since then, a lot of interesting theoretical and experimental work on THz SPPs have been carried out [2-18]. However, the coupling condition of THz SPPs is demanding, and the coupling efficiency has always been low. The coupling problem has become a topic of concern [19-25].

We put forward using double-dielectric-slab waveguide to couple the THz SPPs. We calculate the coupling efficiency, and it is identified that not only the theoretical coupling efficiency is higher but also the loss in the process of coupling is very small. This will drive the development of the THz SPPs researches and applications, and provide theoretical support for the design of THz function devices and realizing the THz biomedical super resolution imaging [26-28].

2. The mode field distribution

2.1 The mode field of odd TM mode of double-dielectric-slab waveguide and Sommerfeld waves

The double-dielectric-slab waveguide is composed of two pieces of silicon slab with a certain interval. The schematic diagram is shown in Fig. 1, the width along *y* direction is supposed to be infinity, and the guided mode is confined to transmit along z direction.

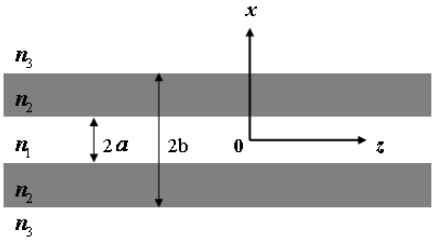

Fig. 1. The double-dielectric-slab waveguide structure

Through derivation, we get the distribution equations of transverse electric field of the odd TM mode as follows:

$$E_x = \begin{cases} A\dfrac{|x|}{x}\sin(h_1 a)\dfrac{(\beta/\omega\varepsilon_3)\cos\alpha}{\cos[h_2(b-a)-\alpha]}\exp[-h_3(|x|-b)] & |x|>b \\ A\dfrac{|x|}{x}(\beta/\omega\varepsilon_2)\sin(h_1 a)\dfrac{\cos[h_2(b-|x|)-\alpha]}{\cos[h_2(b-a)-\alpha]} & a<|x|<b \\ A(\beta/\omega\varepsilon_1)\sin(h_1 x) & |x|<a \end{cases} \tag{1}$$

Where A is a coefficient related with the mode power, $h_1 = (n_1^2 k_0^2 - \beta^2)^{1/2}$, $h_2 = (n_2^2 k_0^2 - \beta^2)^{1/2}$, $h_3 = (\beta^2 - n_3^2 k_0^2)^{1/2}$, $\alpha = \arctan[\dfrac{\varepsilon_2 h_3}{\varepsilon_3 h_2}]$; n_1 , n_2 , n_3 are refraction indices of air, slab and air, respectively, β is the complex propagation constant of the waveguide, and k_0 is the wave number in vacuum. The material of the slab adopts silicon here. The refraction index of air is $n_1 = \sqrt{\varepsilon_1} = n_3 = \sqrt{\varepsilon_3} = 1$, and the refraction index of silicon is $n_2 = \sqrt{\varepsilon_2}$. The relative dielectric constant ε_2 of silicon can be calculated by the Drude model:

$$\varepsilon = \varepsilon_\infty - \frac{\omega_p^2}{\omega^2 - i\omega\omega_\tau} \tag{2}$$

Where $\varepsilon_\infty = 11.7$ is the high frequency dielectric constant of silicon, ω_p is the plasma oscillation frequency, ω_τ is the damping frequency and ω is the angular frequency of the THz wave. Here, we adopt the silicon with low doped degree, and the parameters are: $\omega_p = 0.01\times10^{12}$ Hz , $\omega_\tau = 0.67\times10^{12}$ Hz .

When the interval between the two slabs is $d = 2a = 1$ mm, the slab thickness is $t = 0.0435$ mm, and the THz wave frequency is $f = 0.3$ THz, the mode propagation constant of odd TM mode is gotten to be $\beta = 6283.66 - i*3.9297\times10^{-6}$. According to the propagation

constant and Eq. (1), we get the amplitude distribution of transverse electric field of this mode, as shown in Fig. 2 (a). On either side of x = 0, amplitude of electric field is symmetric (the part of $x < 0$ is not shown). When the diameter of the copper wire is 1 mm, f = 0.3 THz, the distribution of the radial electric field amplitude of TM mode of Sommerfeld waves in the air is shown in Fig 2 (b) [4].

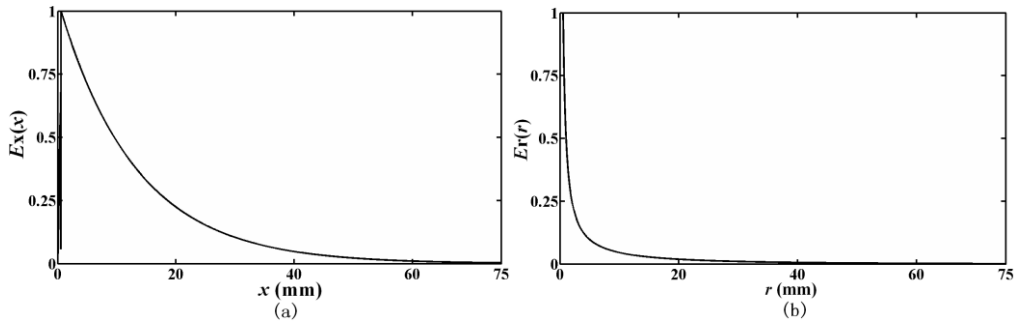

Fig. 2. The normalized amplitude distribution of transverse electric field E_x (a) of the odd TM mode in the double-dielectric-slab waveguide and the normalized amplitude distribution of radial electric field (b) of Sommerfeld waves in the air

The vibration of the transverse electric field of odd TM mode in double-dielectric-slab waveguide is in the opposite direction. The polarization direction is shown in Fig. 3.

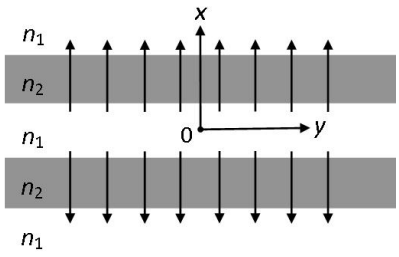

Fig. 3. The polarization direction of transverse electric field of odd symmetrical TM mode in double-dielectric-slab waveguide

2.2 Mode matching analysis

For a cylindrical metal wire, the field intensity of THz SPPs in its internal part can be ignored [1], and the pattern can be regarded as a hollow beam. However, the center of the THz wave in free space is usually of the highest field intensity. Therefore in the coupling of THz SPPs, THz wave corresponding to the part of the wire section cannot be used effectively. However the middle field strength of the odd symmetrical TM mode in the double-dielectric-slab waveguide is very weak, and the amplitude distribution of the transverse electric field is shown in Fig. 2 (a). By comparing Fig. 2 (a) and (b), we see that there is a much higher matching degree in the mode field distribution. Furthermore the vibration direction of the transverse electric field in the double-dielectric-slab waveguide is vertical with respect to silicon slab as shown in Fig. 3, and the vibration directions are of the opposite on both sides of the y axis.

When the given THz frequency is 0.3 THz, silicon interval is $d = 2a$ = 1 mm, the relationships between the loss coefficient and the effective refractive index of odd symmetrical TM mode in the double-dielectric-slab waveguide with the thickness t of the silicon slab is shown in Fig. 4. By the figure, we can see that the loss coefficient of the pattern

in the given thickness range is very small, and its effective refractive index changes continuously from 1 to 2.5. The effective refractive index of THz SPPs of the metal wire is a slightly larger than 1. Through the reasonable design of the thickness of the silicon slab, we can make the matching of the wave vector.

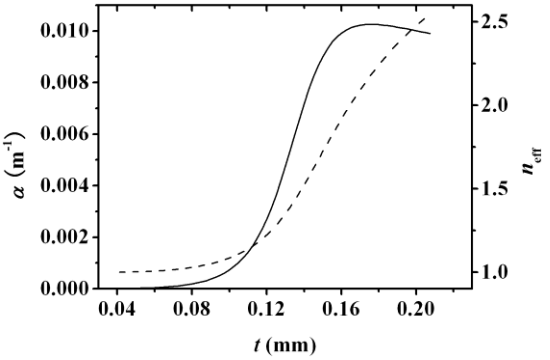

Fig. 4. The dependences of the amplitude loss coefficient (solid line) and effective refractive index (dashed line) of odd symmetrical TM mode in double-dielectric-slab waveguide on the slab thickness *t*.

3. The coupling between odd TM mode field of double-dielectric-slab waveguide and Sommerfeld waves of cylindrical wire

3.1 The equations to calculate coupling efficiency

The mode field distribution of the incident THz beam from double-dielectric-slab waveguide on the *x* direction is shown in Eq. (1). In *y* direction the pattern is a Gaussian distribution, therefore the mode field distribution equation of the incident beam is:

$$\psi_A(x,y)=\begin{cases} A\dfrac{|x|}{x}\sin(h_1 a)\dfrac{(\beta/\omega\varepsilon_3)\cos\alpha}{\cos[h_2(b-a)-\alpha]}\exp[-h_3(|x|-b)]\exp(-\dfrac{y^2}{2\sigma^2}) & |x|>b,-\infty<y<+\infty \\ A\dfrac{|x|}{x}(\beta/\omega\varepsilon_2)\sin(h_1 a)\dfrac{\cos[h_2(b-|x|)-\alpha]}{\cos[h_2(b-a)-\alpha]}\exp(-\dfrac{y^2}{2\sigma^2}) & a<|x|<b,-\infty<y<+\infty \\ A(\beta/\omega\varepsilon_1)\sin(h_1 x)\exp(-\dfrac{y^2}{2\sigma^2}) & |x|<a,-\infty<y<+\infty \end{cases} \tag{3}$$

Where σ is the Gaussian radius. The mode field distribution equation of the cylindrical wire Sommerfeld waves in the air can be written as follows [21]:

$$\psi_B(x,y)=h(k_0{}^2-h^2)^{-1/2}H_1^{(1)}(\sqrt{k_0{}^2-h^2}\sqrt{x^2+y^2}) \tag{4}$$

Where h is the mode propagation constant of the guided mode in copper wire, k_0 is the wave number in vacuum. The projection factor is:

$$\cos\theta=\frac{x}{\sqrt{x^2+y^2}} \tag{5}$$

The coupling efficiency can be calculated as [21, 29]:

$$C=\frac{\left|\int_S \psi_A\psi_B{}^*\cos\theta dS\right|^2}{\int|\psi_A|^2 dS\int|\psi_B|^2 dS} \tag{6}$$

3.2 The relationship between coupling efficiency and the thickness *t* of a silicon slab

When the wire diameter is 1 mm, $d = 2a$ = 1 mm as interval between two silicon slabs, THz frequency is f = 0.3 THz, Gaussian distribution σ = 6.75 mm. We get the law of coupling efficiency with respect to the thickness t of the silicon slab, as shown in Fig. 5:

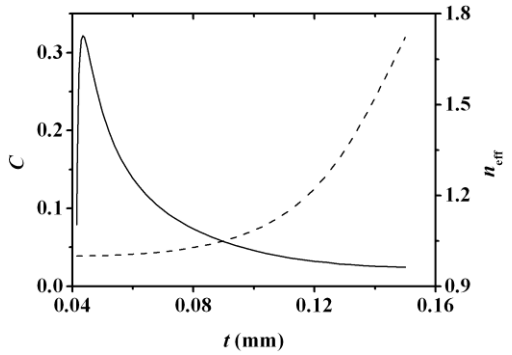

Fig. 5. The dependences of the coupling efficiency (solid line) and the effective refractive index (dashed line) of double-dielectric-slab waveguide on the thickness t of silicon slab

From the figure we can see that there is an optimal thickness of the silicon slab which makes the coupling efficiency to be maximum. At the optimal thickness t = 0.0435 mm, the highest coupling efficiency is up to $\approx$32%. The coupling efficiency first increases sharply and then decreases with the increasing of thickness. This is because when the thickness is lower than the optimal thickness, the mode field radius on x direction of double-dielectric-slab waveguide is too large and the matching degree of mode field distribution is very low. When the thickness is larger than the optimal thickness, the matching degrees of both the wave vector and the mode field distribution are much lower. The highest coupling efficiency has not been appeared at the point where the wave vectors match as exactly. It is a little higher in the double-dielectric-slab waveguide. This is because of the matching degree of the mode field distributions.

3.3 The relationship between the coupling efficiency and the Gaussian radius σ of the *y* direction

For the wire diameter of 1 mm, slabs interval of $d = 2a$ = 1 mm, THz frequency of f = 0.1 THz, 0.3 THz and 1 THz, we get the approximate optimal thicknesses of silicon slab, they are t = 0.202 mm, 0.0435 mm and 0.0054 mm, respectively. We get the rules of the coupling efficiency changing with the Gaussian radius σ of the y direction as shown in Fig. 6:

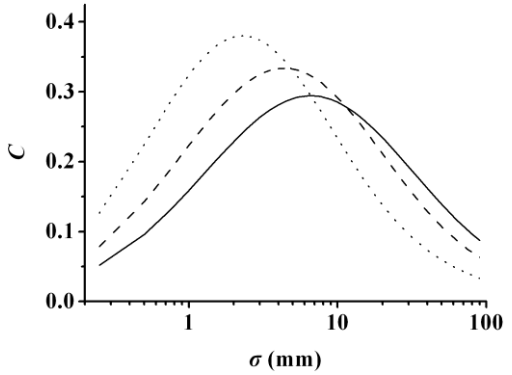

Fig. 6. The dependence of coupling efficiency on the Gaussian distribution radius σ of y direction: f = 0.1 THz, t = 0.202 mm, solid line; f = 0.3 THz, t = 0.0435 mm, dashed line; f = 1THz, t = 0.0054 mm, dotted line.

From the figure we can see that with the increase of σ, the coupling efficiency increases first, and there is an optimal σ for each frequency. At f = 1 THz the maximum coupling efficiency is more than 38%.

3.4 The relationship between coupling efficiency and the THz frequency

For the wire diameter of 1 mm, and $d = 2a$ = 1 mm, σ = 6.75 mm, t = 0.15 mm, we get the rule of the coupling efficiency changing with the THz frequency f as shown in Fig. 7:

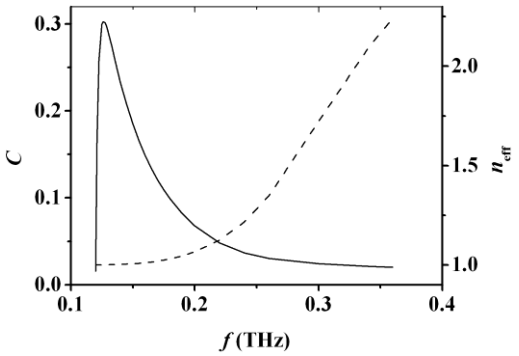

Fig. 7. The dependences of the coupling efficiency (solid line) and the effective refractive index (dashed line) of double-dielectric-slab waveguide on the THz frequency f.

Fig. 7 illustrates that the coupling efficiency has a maximum value with the increase of the THz frequency. For this kind of structure of the double-dielectric-slab waveguide, the maximum coupling efficiency is $\approx$30% at 0.126 THz.

3.5 The relations between maximum coupling efficiency C_{opt} and the optimal slab thickness t_{opt} and optimal Gaussian radius σ_{opt} with THz frequency

In order to achieve for maximum coupling efficiency at a given THz frequency, we need to design the structure of the double-dielectric-slab waveguide and the structure of THz sources beam. The wire diameter is 1 mm, the slabs interval is $d = 2a$ = 1 mm, and we only change t and σ. We get the maximum coupling efficiency and the optimal waveguide and beam structure at different THz frequency as shown in Fig. 8.

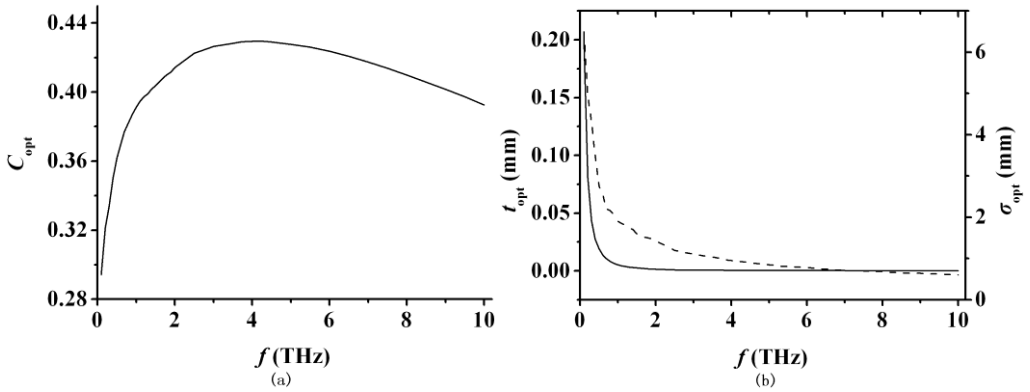

Fig. 8. The laws of maximum coupling efficiency (a) and the optimal thickness of the silicon slab (b, solid line) and the optimal radius of the Gaussian beam (b, dashed line) changing with the THz frequency f.

The maximum coupling efficiency C_{opt} increases first and has a maximum value with the increase of frequency. At 4.2 THz the maximum C_{opt} is $\approx$42.9% when t_{opt} = 0.00039 mm and σ_{opt} = 0.93 mm. The corresponding optimal thickness of the slab and optimal Gaussian radius both decrease on THz frequency as shown in Fig. 9 (b). It is worth to point out that in the range of 1.4 - 9.1 THz, the maximum coupling efficiency C_{opt} is exceed 40%.

3.6 The law of coupling efficiency changing with the slabs interval *d*

In case of *f* = 4.2 THz, wire diameter is 1 mm, σ = 0.93 mm, t = 0.00039 mm, we change the interval *d* between the two slabs, and we get the results below:

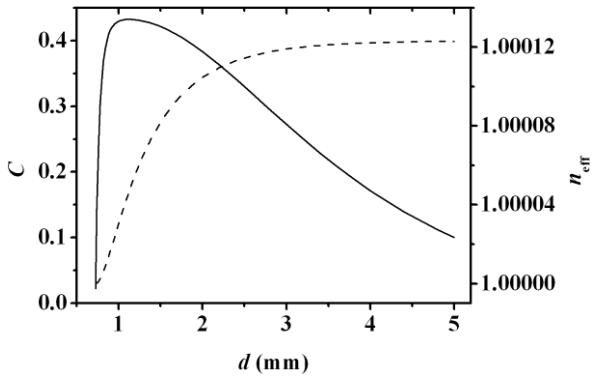

Fig. 9. The dependence of the coupling efficiency (solid line) and the effective refractive index (dashed line) of double-dielectric-slab waveguide on the interval *d* of the two silicon slabs

From Fig. 9, we can see that there exists an optimal *d* of a THz frequency, Optimal *d* for 4.2 THz is about 1.12 mm at this condition, and the maximum coupling efficiency is up to $\approx$43.2%. At last, we change *t*, *d*, and σ at the same time, and we get the maximum coupling efficiency at 4.2 THz is $\approx$43.5%, when t_{opt} = 0.00037 mm, d_{opt} = 1.18 mm, σ_{opt} = 0.92 mm.

4. The stimulation of odd symmetrical TM mode in double-dielectric-slab waveguide

For the cylindrical metal wire THz SPPs, we plan to set up the coupling experiment system as shown in Fig. 10. The SIFIR-50 is the THz source. Since the field component of the TM mode and TE mode is completely orthogonal, by setting the polarization direction of incident THz wave we can only select the TM mode. THz wave first reflects on the metal parabolic mirror to collimate, and then half of the THz wave directly exposes to the double-dielectric-slab waveguide, and the other half first pass through the $\lambda/2$ medium slice and then exposes to the double-dielectric-slab waveguide. This make the incident THz wave in the waveguide to have a odd symmetrical distribution, which can inspire odd symmetrical TM mode.

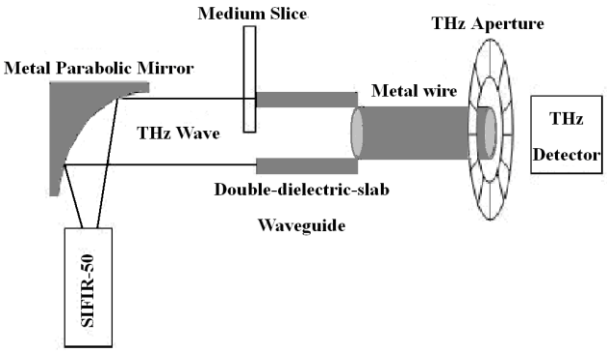

Fig. 10. The planning coupling experimental system

5. Conclusion

We propose using odd TM mode of double-dielectric-slab waveguide to implement the coupling of cylindrical wire Sommerfeld waves. We analyze the mode matching issue. The calculation formulas of coupling efficiency are given, and we calculate the rules of the coupling efficiency changing with the silicon thickness *t*, Gaussian radius σ of *y* direction and the THz frequency. We further obtain the laws of the maximum coupling efficiency C_{opt} and the t_{opt} and σ_{opt} changing with the frequency when *d* is equal to the wire diameter. Finally we change the slabs interval *d*, and we find the maximum coupling efficiency. The maximum coupling efficiency we calculate is as high as 43.5% at 4.2 THz. We further give the planning experiment system and this scheme has many advantages in the experiment. We can realize much higher experimental coupling efficiency of metal wire THz SPPs.

Acknowledgement This work is supported by the Specialized Research Fund for the Doctoral Program of Higher Education of China (Grant No. 20134408120002) and the Fund Project for Shenzhen Fundamental Research Programme (Grant No. JCYJ20130329140707824).

References

[1] K.Wang, and D. M. Mittleman, Metal wires for terahertz waveguiding, Nature **432**, 376 (2004).

[2] K. Wang, and D. M. Mittleman, Dispersion of surface plasmon polaritons on metal wires in the terahertz frequency range, Phys. Rev. Lett **96**, 157401 (2006).

[3] T. Jeon, J. Zhang, and D. Grischkowsky, THz Sommerfeld wave propagation on a single metal wire, Appl. Phys. Lett **86**, 161904 (2005).

[4] Q. Cao, and J. Jahns, Azimuthally polarized surface plasmons as effective terahertz waveguides, Opt. Express **13**, 511 (2005).

[5] X. He, J. Cao, and S. Feng, Chin. Simulation of the propagation property of metal wires terahertz waveguides, Phys. Lett **23**, 2066 (2006).

[6] R. Zhong, W. Liu, J. Zhou, and S. Liu, Chin. Surface plasmon wave propagation along single metal wire, Phys. B **21**, 393 (2012).

[7] Z. Wang, Y. Zhang, R. Xua, W. Lin, Investigation of THz Sommerfeld wave propagation on single-wire at different temperature, Optik **123**, 2159 (2012).

[8] J. Yang, Y. Niu, G. Lin, Y. Qi, and S. Gong, Chin. Zero-dispersion waveguide of sub-skin-depth terahertz

plasmons using metallic nanowires, Opt. Lett **11**, 082401 (2013).
[9] D. K. Gramotnev, and S. I. Bozhevolnyi, Plasmonics beyond the diffraction limit, Nat. Photonics **4**, 83 (2010).
[10] S. A. Maier, S. R. Andrews, L. Martı´n-Moreno, and F. J. Garcı´a-Vidal, Terahertz surface plasmon-polariton propagation and focusing on periodically corrugated metal wires, Phys. Rev. Lett **97**, 176805 (2006).
[11] H. Liang, S. Ruan, and M. Zhang, Terahertz surface wave propagation and focusing on conical metal wires, Opt. Express **16**, 18241 (2008).
[12] V. Astley, R. Mendis, and D. M. Mittleman, Characterization of terahertz field confinement at the end of a tapered metal wire waveguide, Appl. Phys. Lett **95**, 031104 (2009).
[13] X. Y. He, Investigation of terahertz Sommerfeld propagation along conical metal wire, J. Opt. Soc. Am. B **26**, A23 (2009).
[14] H. Liang, S. Ruan, M. Zhang, H. Su, Nanofocusing of terahertz wave on conical metal wire waveguides, Opt. Commun **283**, 262 (2010).
[15] M. Awad, M. Nagel, and H. Kurz, Tapered Sommerfeld wire terahertz near-field imaging, Appl. Phys. Lett **94**, 051107 (2009).
[16] J. Yang, Q. Cao, and C. Zhou, Theory for terahertz plasmons of metallic nanowires with sub-skin-depth diameters, Opt. Express **18**, 18550 (2010).
[17] X. He, Investigation of terahertz surface waves of a metallic nanowire, J. Opt. Soc. Am. B **27**, 2298 (2010).
[18] E. Verhagen, M. Spasenović, A. Polman, and L. K. Kuipers, Nanowire plasmon excitation by adiabatic mode transformation, Phys. Rev. Lett **102**, 203904 (2009).
[19] H. Cao, and A. Nahata, Coupling of terahertz pulses onto a single metal wire waveguide using milled grooves, Opt. Express **13**, 7028 (2005).
[20] A. Agrawal, and A. Nahata, Coupling terahertz radiation onto a metal wire using a subwavelength coaxial aperture, Opt. Express **15**, 9022 (2007).
[21] L. Chusseau, and J.-P. Guillet, Coupling and propagation of Sommerfeld waves at 100 and 300 GHz, J. Infrared Millim. Terahz Waves **33**, 174 (2012).
[22] A. Edelmann, L. Moeller, and J. Jahns, Coupling of terahertz radiation to metallic wire using end-fire technique, Electron. Lett **49**, 884 (2013).
[23] J. A. Deibel, K. L. Wang, M. D. Escarra, and D. M. Mittleman, Enhanced coupling of terahertz radiation to cylindrical wire waveguides, Opt. Express **14**, 279 (2006).
[24] W. Zhu, A. Agrawal, H. Cao, and A. Nahata, Generation of broadband radially polarized terahertz radiation directly on a cylindrical metal wire, Opt. Express **16**, 8433 (2008).
[25] Z. Zheng, N. Kanda, K. Konishi, and M. Kuwata-Gonokami, Efficient coupling of propagating broadband terahertz radial beams to metal wires, Opt. Express **21**, 10642 (2013).
[26] A. R. Orlando, and G. P. Gallerano, Terahertz radiation effects and biological applications, J. Infrared. Milli. Terahz. Waves **30**, 1308 (2009).
[27] M-A. Brun, F. Formanek, A.Yasuda, M. Sekine, N. Ando, and Y. Eishii, Terahertz imaging applied to cancer diagnosis, Phys. Med. Biol **55**, 4615 (2010).
[28] H. Chen, W.-J. Lee, H.-Y. Huang, C.-M. Chiu, Y.-F. Tsai, T.-F. Tseng, J.-T. Lu, W.-L. Lai, and C.-K. Sun, Performance of THz fiber-scanning near-field microscopy to diagnose breast tumors, Opt. Express **19**, 19523 (2011).
[29] J.A.Arnaud, Beam and Fiber Optics (Academic Press, 1976)